1.3 TURBULENCE SPECTRA ABOVE THE SURFACE FRICTION LAYER IN A CONVECTIVE BOUNDARY LAYER

K.G. McNaughton, R. Clement and J.B. Moncrieff
School of GeoSciences, University of Edinburgh, Scotland

1. INTRODUCTION

For modeling purposes the convective boundary layer (CBL) is usually divided into horizontal layers, each defined by the scaling parameters which reduce the layer's turbulent statistics to universal values or relationships (e.g. Holtslag and Nieuwstadt, 1986). We will be concerned with the `local free convection layer', which lies above the surface friction layer and extends upwards to the bottom of the mixed layer at about 0.1 z_i, where z_i is inversion height. In this layer many turbulence quantities have approximately constant values when scaled using height, z, and the free-convection velocity scale, $u_f = \left(g z \overline{w'\theta'}\right)^{1/3}$. (Undefined symbols have their usual significances.) This layer was first predicted by Obukhov (1946) and Priestley (1954), using dimensional arguments. Its existence is well supported by measurements (Wyngaard et al., 1971; Kaimal et al, 1976).

Though well accepted, this local free convection layer raises an interesting question. Why does free-convection scaling work down to different levels for different quantities? It extends down to ~2.5|L| for the dissipation rate for turbulence kinetic energy (Kader and Yaglom, 1990), where L is the Obukhov length, but to only 1/25th that height for the temperature gradient, variance and dissipation rate (Priestley, 1955; Kader and Yaglom, 1990). For temperature it works down to a level where local free convection does not occur, at least not in the sense of plumes of warm air rising autonomously by the action of their own buoyancy (McNaughton, 2006). We have more to learn about 'local free convection'.

We first present a re-interpretation of scaling in the outer parts of the CBL, based on the turbulence structure and kinetic energy balance of the CBL. Next we report velocity spectra recorded in a convective boundary layer at heights where 2|L| < z << z_i. The measurements were made over a smooth playa surface in Western Utah. The spectra are generally consistent with the classic results from Minnesota (Kaimal et al., 1976), but compared to them we find extra velocity variance at high wavenumbers, increasing towards the ground, and reduced variance at some smaller wavenumbers, with reduction increasing with height. We discuss these results in terms of the turbulence and energy processes in the CBL.

Corresponding author address: K.G. McNaughton, School of GeoSciences, University of Edinburgh EH9 3JN;.e-mail keith.mcnaughton@ed.ac.uk

2. ENERGY SCALING OF SPECTRA

The scientific background to our experiment is the scaling theory of 'local free convection', as given by Wyngaard et al. (1971), and the experimental results and analysis from the Minnesota experiment reported by Kaimal et al. (1976). In this section we revise these classic scaling results by considering the kinetic energy balance of the whole CBL, treating it as a whole self-organized system rather than as the product of independent local processes. We deduce reference spectra that can serve as a standard of comparison for our own results, which will be presented in section 5, below.

Reference spectra are defined here as spectra that have the scaling properties reported by (Kaimal et al., 1976) for the Minnesota results and extended consistently to vertical velocity spectra. Reference u and v spectra collapse when lengths are scaled on z_i and energies on $\left(z_i \varepsilon_o\right)^{2/3}$, and reference w spectra collapse when these are scaled on z and $\left(z \varepsilon_o\right)^{2/3}$. This merely appropriates the Minnesota result, but notice that Kaimal et al. write their scaling factor for u and v spectra as $w_*^2 \psi^{2/3}$, where w_* is the Deardorff convective velocity scale (Deardorff, 1970) and ψ is a dimensionless dissipation rate. Appeal to definitions shows that $w_*^2 \psi^{2/3}$ is identical to what we write as $\left(z_i \varepsilon_o\right)^{2/3}$. The u and v power spectra have peaks whose positions scale on z_i while the w-spectra have peaks whose positions scale on observation height, z.

The shapes of the Minnesota spectra are significant. The u and v spectra have a single peak at z_i-scale, followed by a region with a -2/3 slope on a log-log plot that extends from near there all the way up to very high wavenumbers. These -2/3 regions do not wholly represent inertial sub-ranges, despite their slopes, because turbulence can not be isotropic when κz < 1. Eddies of this size extend down to the ground, which blocks their vertical motion. Even so, the -2/3 slopes are related to an inertial subrange. The u and v spectra at Minnesota did not change with height, so the -2/3 regions nearer the ground are the same as those found at mid levels of the CBL. At that level the turbulence is isotropic and the -2/3 slopes are diagnostic of a true inertial subrange. That is, the shape of the near-ground spectra appears to be dictated by the Kolmogorov law for the outer turbulence. We are led to propose that the near-surface turbulence represents the effects of eddies from the outer inertial subrange impinging onto the ground, so the near-surface turbulence is fully characterized by parameters taken from the outer turbulence.

We can make some deductions from the spectra at mid levels in the CBL. Their simple structure with a peak followed by an inertial subrange tells us that all the kinetic energy is produced at the scale of the main convective circulations and none at larger wavenumbers. We know this because an inertial subrange is a purely transmission region of a spectrum; one where kinetic energy is neither created nor destroyed. The reason why kinetic energy enters only at the largest scales is that buoyant production of kinetic energy, $g\,\overline{w'\theta'}/T$, is overwhelmingly associated with the organized thermals of the main convection. Smaller parcels of warmer air exist at smaller scales, but these are swept along in the main convective circulations and do not rise except as part of the overall pattern of the main convective circulation.

It has been common practice to parameterize the energy of this main convection using the buoyancy flux. However, buoyancy does not act alone. It is but one term, albeit often the dominant one, in the whole turbulence kinetic energy budget of the CBL. Turbulence kinetic energy is produced by shear at the top of the CBL, and is lost as work done against drag at the ground and as work done against buoyancy during entrainment through the capping inversion. Sharp topography can also transfer large amounts of kinetic energy from the mean flow to the turbulence within the boundary layer. Though these influences may be difficult to assess individually, they all contribute to the net production of turbulence kinetic energy. Net production is balanced by the net dissipation rate, ε_0, so the dissipation rate parameterizes the velocity scale. This direct connection between velocity scale and dissipation rate is why the Minnesota practice of matching inertial subranges is the correct procedure, while their expression of this scale as an adjusted Deardorff velocity is misleading. The Deardorff velocity scale is correct only when

$$\varepsilon_o \approx \frac{g}{2T}\,\overline{w'\theta'} \qquad (1)$$

which is to say, only when buoyant production dominates over all other sources of turbulence kinetic energy in the CBL. Buoyant production did dominate on most occasions at Minnesota, but this domination cannot be guaranteed everywhere. In the general case $(z_i\,\varepsilon_o)^{1/3}$ is the correct convective velocity scale, not the Deardorff scale.

Nearer the ground the horizontal spectra mimic the mid-CBL spectra, so here again ε_0 fully parameterizes the kinetic energy of the eddies. Once again the local buoyancy forces produce no kinetic energy at the scale of the local eddies. Exactly the same conclusion was reached by McNaughton (2006) for turbulence in the unstable surface friction layer, and there the main evidence was quite direct. Buoyant production in the surface layer is directly offset by pressure transport terms of the kinetic energy budget, indicating the buoyancy forces are directly opposed by pressure reaction forces. Thus there is a consistent case that the various sources and sinks of turbulence kinetic energy combine to power the whole flow of the CBL, with the large-scale organization as its dominant feature. The flow near the ground is an integral part of the whole, and local buoyancy makes no local contribution to the local kinetic energy balance at finer scales. That is, the layer where $z_s << z << z_i$, is not a 'local free convection layer'.

The theme of whole-system control of local processes continues when we turn to *w* spectra. Our model is of outer eddies impinging against the ground, but when $z << z_i$ the largest outer eddies, for which $\kappa z_i \sim 1$, are blocked by the ground and so contribute very little energy to the *w* spectrum. Thus z_i is not a relevant length scale for vertical motions where $z << z_i$. The significant eddies lie entirely within the span of the outer inertial subrange. This subrange has no intrinsic length scale, so we must look for one elsewhere. We expect eddies of height ~2 z to contribute most effectively to the *w* spectrum, so observation height, *z*, should scale the peak wavenumber. Outer subrange eddies of that size have energies that scale as $(\varepsilon_o/\kappa)^{2/3}$, so energy of the *w* spectra should scale on $(z\ \varepsilon_o)^{2/3}$. Notice that, unlike the 'free convection' model, our scaling is not just a dimensional result; it is a consequence of Kolmogorov's law for inertial subranges, which gives both the ε_0 parameter and the 2/3 power to this new convective velocity scale. Dimensional consistency is just a necessary adjunct.

We can also predict the asymptotic behavior of the *w* spectrum at small wavenumbers from the outer inertial subrange. Inertial subranges have eddies that are statistically self-similar under scale remappings when energies are scaled on $(\varepsilon_o/\kappa)^{2/3}$. This translates to a statistical self-similarity of impinging eddies. The impinging eddies are also 'attached to the ground', in the sense that their shape is determined by interaction with the ground. McNaughton (2004a) has shown that such turbulence produces power spectra that approach an asymptote with +1 slope at small wavenumbers. This asymptote was not observed at Minnesota, probably because the velocity signals were hi-pass filtered before analysis.

3. EXPERIMENTAL

Turbulence measurements were made over an extensive playa surface at the SLTEST site in Western Utah from 23 May to 3 June 2005. Results reported here are from an array of eighteen North-facing CSAT3 sonic anemometers (Campbell Scientific). Nine of these were mounted on a tower at 1.42, 2.05, 3.00, 4.29, 6.13, 8.77, 12.5, 17.9, and 25.6 meters above ground. The other nine were mounted on tripods in a cross-wind line, set variously at 3.00 meters height with 10-meter spacing, 2.05 meters height with 10-meter spacing or 2.05 meters height with 3-

meter spacing. This horizontal array was installed principally to serve another experiment but we use this data, averaged across the Western-most 6 anemometers, to provide the site heat flux and averaged spectra to cross-check the tower spectra at one level.

Figure 1. Array of CSAT3 sonic anemometers at the SLTEST site in May, 2005. The instruments were placed forward of a raised causeway, giving about 100 km of unobstructed fetch for winds from Northerly directions.

Precipitation had been higher than usual in the seasons preceding the experiment, resulting in a high water table, very smooth surface and an energy balance that favored a basin circulation bringing winds from the North, in which direction the surface was uniform for about 100km. The site is described by Klewicki et al. (1995). Fig. 1 shows the site and the array of sonic anemometers.

All the CSAT3 anemometers had been factory-calibrated in still air in the year preceding the experiment, most in the month preceding the experiment. Data were collected at 20Hz. Sampling was synchronized across the entire array using three CR5000 data loggers (Campbell Scientific) connected in a master-slave configuration. Thus the wider experimental design allowed for analysis of turbulent structures passing through the entire array.

A crane was used to access the tower and mount the CSAT3 anemometers. This allowed us to level them to within ±0.5˚.

The playa was very wet at the time the tower was erected, so trucks could not drive out onto its soft surface. As a result the tower was erected close to the raised berm where our trailers were parked (see Fig. 1). The berm surface was 0.8 m above the playa surface, and our tower was erected 6 meters from its North-West corner. This caused some flow distortion at the tower. The six sonic anemometers in the horizontal array to the West of the tower gave very uniform results, but comparisons between these and instruments on the tower at the same level showed that mean wind speed at 3 meters on the tower was reduced about 6% for Northerly winds. Comparisons of spectra show much smaller effects, being insignificant in the results reported here.

4. DATA SELECTION AND PROCESSING

We selected 69 runs of half an hour each from highly-convective periods when winds were from the North and the modulus of the Obukhov length, $|L|$, was less than 2 meters. This means that the depth of the surface friction layer, given by

$$z_s = \left(u_*^3 + \overline{v_*^3}\right) \Big/ k\varepsilon_O \qquad (2)$$

(McNaughton, 2004b, 2006) was less than about 4 meters, assuming $z_s \sim 2|L|$ (McNaughton, 2004b). For these runs at least the top six sonic anemometers were above the surface friction layer. All anemometers lay within the bottom tenth of the boundary layer, assuming 1 km for the inversion height, z_i.

In view of the accuracy of the anemometer placement and the extreme flatness of the site, we applied no co-ordinate rotations to our data beyond a horizontal rotation to set the x direction into the mean wind for each run. Results showed a systematic variation of apparent wind elevation angle with wind direction, up to 1.5˚ for winds along the instrument axis. This pattern was similar for all instruments, regardless of height. We interpret this apparent angle as an artifact caused by non-ideal instrument response. Such errors should not be corrected by co-ordinate rotation. Roland Vogt and his colleagues have calibrated several CSAT3 anemometers for elevation angles out to ±35˚ (personal communication, 2005). We tried using their average calibration to correct our results. This altered the directional patterns of apparent elevation angles but did not systematically remove the effect. We therefore used the unmodified factory calibrations to calculate the spectral results reported here. We believe the results and interpretations presented here are robust with respect to calibration uncertainties.

We used Taylor's frozen-turbulence hypothesis to convert from frequency to wavenumbers in all our results, using $\kappa = 2\pi f/U_{25.6}$ where f is frequency and $U_{25.6}$ is the mean wind speed at our top level at 25.6 meters. Taylor's frozen turbulence assumption is problematic because it cannot properly accommodate coherent eddies in sheared flows. We used U_{26} as a best estimate of the mean wind speed in the CBL. Our conversion assumes that turbulence through the whole CBL moves as a single frozen block at speed $U_{25.6}$. This correctly registers the main peaks in the u and v spectra observed at all heights on the κz_i axis. Even so, we expect very small eddies to travel with the local wind at each height, so we should use $\kappa = 2\pi f/U_z$ to calculate wavenumbers where $\kappa z > 1$. For the runs selected here the average value of $U_{25.6}/U_{1.42}$ is only 1.25, so conversions from frequency to wavenumbers are secure to within this tolerance. Any uncertainty has negligible effect on the interpretation of our results.

We used the splicing procedures described by Kaimal and Finnigan (1994) to calculate spectra. Data for high frequency subsets had means removed before windowing while the low frequency set was detrended before windowing. The scaling parameters for each run were obtained from the *u* spectrum at the top of the tower. These were then used to scale all spectra from that run. Scaled spectra were then averaged at each level across all runs. This gave 9 sets of spectra: one from each level. Any differences found in spectra from different heights is a direct expression of the raw data, with no artifacts introduced by different treatments of the data at different levels.

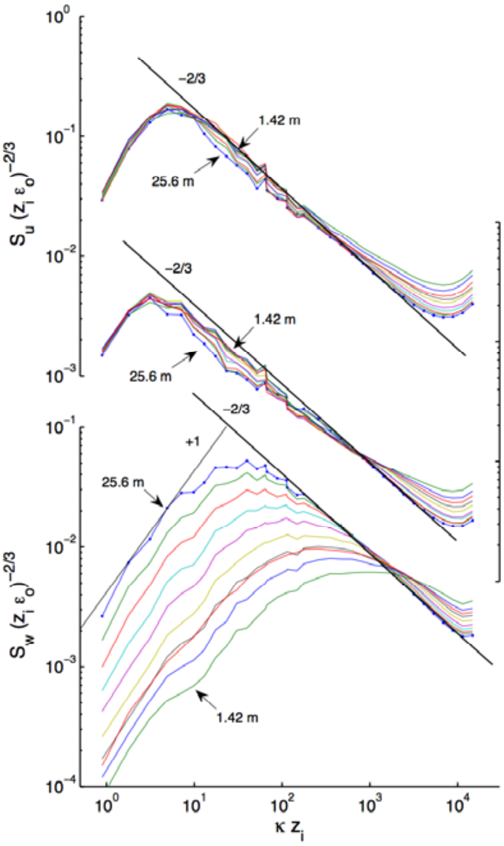

Figure 2. Power spectra for *u* (top), *v* (middle) and *w* (bottom) components of the wind averaged for each of the 9 levels on the tower at the SLTEST site. All data are from unstable conditions with $|L| < 2$ meters, where L is the Obukhov length. Results are plotted on outer-scaled axes (see text) so the *u* and *v* spectral peaks for each level are in the same position. The lines marked '-2/3' indicate the Kolmogorov law for inertial subranges. The +1 line on the *w* spectra indicates the slope of the expected asymptote for a population of self-similar attached eddies. Also shown (red lines) are the averaged spectra from the 6 Western-most anemometers of the horizontal array at 3 meters. These spectra differ little from the tower results at the same height (grey lines). Color coding is indicated on the bottom plot, with the anemometer levels in sequence from highest at 25.6 m (blue) down to lowest at 1.42 m (green). The same sequence is used on the other plots.

For each run we calculated ε_o from the plateau region of the *u* spectrum at 25.6 meters, plotted as

$$\kappa^{5/3} F_u(\kappa) = \alpha_1 \varepsilon_o^{2/3} \quad (3)$$

where $\alpha_1 = 0.5$, as recommended by Sreenivasan (1995). The inversion height was estimated using the Minnesota relationship, $z_i = \lambda_m/1.5$ where λ_m is the wavelength of the maximum of the pre-multiplied *u* spectrum at 25.6 meters.

5. RESULTS

Averaged spectra from the SLTEST site are shown in Figs. 2 and 3. Each spectrum is an average over all 69 runs. Close agreement between the tower result at 3 meters and the corresponding result from the six most Westerly anemometers of the horizontal array indicates that these results are not significantly affected by flow distortion at the tower.

Also shown on Figs. 2 and 3 are -2/3 lines, representing Kolmogorov's law for inertial subranges. These lines, which indicate the behavior of our reference spectra in his range, fit the observed spectra reasonably well, and for the *u* and *v* spectra this fit extends over a three-decade range of wavenumbers. However, our spectra also deviate from the reference in systematic ways. Our spectra have more energy than reference spectra at large wavenumbers, even after allowing for aliasing near the sampling frequency. This is evident in all three components, and its amount increases systematically as height decreases.

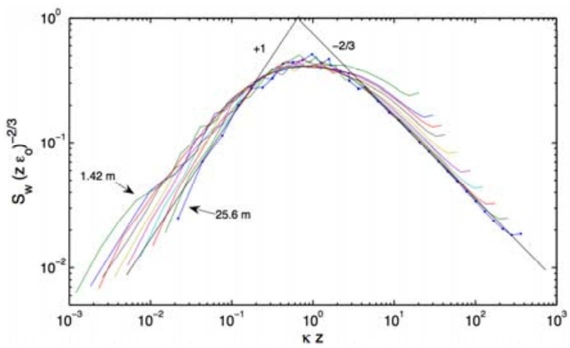

Figure 3. Spectra of vertical velocity fluctuations normalized using $(z\varepsilon_o)^{2/3}$ and plotted against κz. Also shown is the -2/3 line showing the slope of predicted inertial subrange of the reference spectrum, and the +1 line showing the slope of the predicted asymptote to the reference spectrum. Colour coding of levels is the same as in Fig. 2.

The situation is reversed at smaller wavenumbers, near $\kappa z_i = 20$ or, alternatively, near $\kappa z = 0.1$. The *u* and *v* spectra from the lowest anemometer follow the reference spectrum most closely in this region while those from higher levels have progressively less energy. Energy reduces by about one third as height increases from 1.42 to 25.6 meters. The *u* and *v* spectra converge towards the peak, and display the same (universal) behavior at the peak. Good spectral collapse at the peaks gives confidence that the differences found at larger wavenumbers are real.

The w spectra have peaks at $\kappa z = 0.6$, so the eddies contributing most to these spectra have wavelengths, λ_m, about ten times observation height. Such eddies have a 5:1 length to height ratio. This compares with 1:1 ratio for shear turbulence low in the surface friction layer, and 6:1 above the friction layer $-z/|L| > 1.5$, both values being from the Kansas experiment (Kaimal et al., 1972).

6. DISCUSSION

We will discuss separately the 'extra' energy at larger wavenumbers and the 'missing' energy at smaller wavenumbers. This is justified because this is not just a spectral redistribution of energy: the energy 'missing' at small wavenumbers far exceeds the 'extra' energy at large wavenumbers, though the log scale used in Fig. 2 tends to disguise this.

6.1 'Extra' energy at large wavenumbers

The rate of turbulence kinetic energy production is larger near the ground, within the surface friction layer, than it is above. This surface layer would sometimes have grown to engulf the lowest three anemometers, which would then have sampled the extra turbulence kinetic energy to be found there. Thus they display extra energy at large wavenumbers. However, we found extra energy all the way up to 25.6 meters, to more than 6 times the height of the surface layer, and this extra energy reduced systematically over the whole range, not showing any sign of a definite cut-off level. We conclude that the excess energy must have been lifted from the surface layer where it was produced and transported up to various higher levels by an organized turbulence process.

This conclusion implies a major modification of the model of the surface friction layer described by McNaughton (2006). In that model the outer turbulence drives the surface friction layer by acting horizontally at its top. We now propose that the outer eddies reach down to, and drag along the ground. That is, the surface shear processes act within the lowest parts of the outer eddies, not beneath them. The surface friction layer is then not a distinct layer but an average over local events occurring in the bottoms of many large eddies.

Our experiment gives no direct information on the form of these outer eddies or how they might transport finer-scale eddies up from the surface layer, but we can make a suggestion based on results from many sources. We propose that these outer eddies are pairs of counter-rotating stream-wise vortices, such as can be constructed from field data using empirical orthogonal functions (Zhuang, 1995). Rotating eddies like this, with heights an order of magnitude greater than z_s, could sweep up air from within the surface layer and carry it aloft in the form of sheet plumes. This mechanism has been described by Mehta and Bradshaw (1988). Sheet plumes have been observed in Rayleigh-Bénard cells in the laboratory (Puthenveettil and Arakeri, 2005) and from low-flying aircraft, where they appear as warm updraft structures aligned with the wind (Laubach and McNaughton, unpublished observations 2005). Infrared imaging of surface temperature shows linear striations (Derksen, 1974), suggesting that there are whole arrays of such structures rather than isolated pairs.

There are several indirect lines of evidence that also support this hypothesis. One is that the 'extra' kinetic energy here solves the problem of 'missing' kinetic energy in the surface layer that McNaughton (2006) identified as a problem with his model. The driven-from-the-top model could not explain why the dissipation rate (calculated from the kinetic energy at fine scales) is typically smaller than the neutral value, $u_\varepsilon^3 / kz\varepsilon$, when $-z/L \sim 0.2$. Our revised model explains that this missing energy is swept up, as the energy of included fine-scale eddies, in the plumes along with heat and other scalars. Technically, McNaughton wrongly neglected a cross-scale interaction term in his kinetic energy budget for the surface layer, this term being $\overline{\tilde{w}e''}$ where $\tilde{w}$ is the vertical velocity associated with the outer eddy motion and e'' is the fluctuating the kinetic energy of the fine-scale eddies originating in the surface layer.

Another line of evidence is that of scalar spectra from the surface layer that show evidence of an interaction between inner-scale and outer-scale processes (McNaughton and Laubach, 2000; McNaughton and Brunet, 2002). The present model proposes that heat is entrained into the outer eddies by the shear turbulence created as the outer eddies drag along the ground; the outer eddies also rotate and so sweep this heat upwards, along with any scalar substances and small-scale eddies created by the surface friction. The transport thus relies jointly on an inner-scaled process which 'loads heat onto the conveyer belt' and an outer-scale process which provides the 'conveyer belt'. Once lofted, still larger outer eddies repeat the process and carry the heat to greater heights, and so on.

This model also helps us understand the results of Kader and Yaglom (1990). They point out that mean temperature gradient, temperature variance and temperature dissipation all obey 'free convection scaling' down to about $0.05|L|$, which is deep within the surface layer. At this level powerful shear turbulence is produced within the larger outer-scale eddies. Here the majority of the momentum is carried by TEAL cascades, but energy is constantly being redistributed by pressure within these cascades, so it is plausible that scalars get left behind and are transported rather inefficiently. Pressure redistribution within these eddies acts to preserve the form of these eddies against the shear (Zhuang, 1995) so creating continuous larger-scale motions ('conveyer belts') that can transport scalars much more efficiently, despite their smaller vertical velocities.

6.2 'Missing' energy at smaller wavenumbers

Energy is missing from the *u* and *v* spectra in the range $1 < \kappa z_i$ and $\kappa z < 0.7$, the latter limit being the position of the *w*-spectrum peak. The amount missing increases with height, and it amounts to about one third of the reference energy at some wavenumbers. This has not previously been observed, and it is rather curious. We expect spectra in mid CBL to have the reference form because spectra at that level have true inertial subranges and closely follow Komogorov's -2/3 law. The spectra nearest the ground do follow the reference form very well, giving confidence in the measurements, even though these are not true inertial subranges. It is at the heights in between that the spectral energy goes missing.

A theme of this paper is that velocity scaling should not simply be based on dimensional analysis (though this may often give the right answer) but on the kinetic energy budget of the flow. We might therefore expect a well-constructed energy scale to collapse spectra of total energy to a universal form. The spectra energy in Figs. 2 and 3 represent only the kinetic fraction of the total energy, and it neglects other possible forms of energy. In particular it does not represent the pressure potential energy. Our suggestion is that total spectral energy is not missing altogether; it just exists in a form not represented in Figs. 2 and 3.

Since this is an equilibrium flow we expect total energy to be distributed rather evenly, which is to say we expect the sum of kinetic and pressure potential energies, $e+p$, to be uniformly distributed. We expect that the even distribution should apply at each wavenumber as well. We recall that our reference spectra have spectral kinetic energy evenly distributed with height.

We know of no previous work on pressure in this context, but the results of McNaughton (2006) can give some guidance. In the surface friction layer buoyancy forces are opposed by pressure reaction, so buoyancy makes no local contribution to the local kinetic energy budget. In the present context, we may understand this as the main circulation opposing the rise of plumes in the subsidence regions while the horizontal flow near the ground sweeps them in laterally towards the roots of the main thermal updrafts. The subsidence velocity, and so the opposing pressures would increase with height through the plume layer. Higher up there would be no plumes to oppose and so no role for these pressure fluctuations. Thus this explanation is generally consistent with the main properties of the observations. This needs to be investigated further.

7. CONCLUSIONS

The spectra observations presented here appear to be of extraordinarily high quality. Rather than summarize the detailed discussions above, we draw some general conclusions from our interpretation of them.

• Velocity scaling is energy scaling. We show that energy scaling leads to a convective velocity scale for CBLs that is different to the Deardorff scale. The new scale should work better, and work over a wider range of conditions, than the Deardorff scale.

• In CBLs the buoyant energy is all produced at the scale of the main circulations. Buoyancy finds no local expression near the ground except at the full scale of the main circulation. This conclusion reinforces and extends a similar conclusion reached by McNaughton (2006) for unstable surface layers. This means that the Obukhov length scale is not a correct length scale when characterizing near-ground convection.

• Progress from the ground up to higher levels involves a transition from levels where inner-scaled turbulence dominates transport up to levels where outer-scaled turbulence dominates. Parameters of the inner-scale turbulence are u_ε, as defined in (2), with z. Parameters of the outer-scaled turbulence are ε_0 with z_i or z for horizontal or vertical motions, respectively. The scale height for the transition is $z_s = u_\varepsilon^3/k\varepsilon_0$. The scale factor and manner of the transition from inner-dominate to outer-dominated behavior will depend on the particular quantity, but will be a function of z/z_s in every case.

• These considerations led us to a new similarity model. For vertical transport and much else the relationships of the new model are similar in form to those of the Monin-Obukhov similarity theory, but with u_ε replacing u_* and z_s replacing $-L$. Despite this formal similarity, the new scheme is based on a whole-system model that is completely different to the local model that underpins the Monin-Obukhov similarity theory.

Acknowledgements

We thank Prof. Joe Klewicki of the University of Utah for the invitation to participate in the 2005 SLTEST experiment. We also thank Ed Swaitek and Bert Tanner of Campbell Scientific for assistance that went far beyond the terms of the contract when setting up the experiment.

REFERENCES

Deardorff, W.J., 1970: Preliminary results from numerical integrations of the unstable boundary layer. *J. Atmos. Sci.*, **27**, 1209-1231.

Derksen, W.J., 1974: Thermal infrared pictures and the mapping of microclimate. *Neth. J. Agric. Sci.*, **22**, 119-132.

Holtslag, A.A.M. and F.T.M. Nieuwstadt, 1986: Scaling the atmospheric boundary layer. *Bound.-Layer Meteorol.*, **36**, 201-1209.

Kaimal, J.C. and J.J. Finnigan, 1994: Atmospheric boundary layer flows. *Oxford University Press*,

Kaimal, J.C., J.C. Wyngaard, Y. Izumi and O.R. Coté, 1972: Spectral characteristics of surface-layer turbulence. *Quart. J. Roy. Meteorol. Soc.*, **98**, 563-589.

Kaimal, J.C., J.C. Wyngaard, D.A. Haugen, O.R. Coté, Y. Izumi, S.J. Caughy and C.J. Readings, 1976: Turbulence structure in the convective boundary layer. *J. Atmos. Sci.*, **33**, 2152-2169.

Kader, B.A., and A.M.Y. Yaglom, 1990: Mean fields and fluctuation moments in unstably stratified turbulent boundary layers. *J. Fluid Mech.*, **212**, 637-662.

Klewicki, J.C., M.M. Metzger, E. Kelner, E.M Thurlow, 1995: Viscous sublayer flows at R_θ =1 500 000. *Phys. Fluids*, **7**, 857-863.

McNaughton, K.G., 2004a: Attached eddies and production spectra in the atmospheric logarithmic layer. *Bound.-Layer Meteorol.*, **111**, 1-18.

McNaughton, K.G., 2004b: Turbulence structure of the unstable atmospheric surface layer and transition to the outer layer. *Bound.-Layer Meteorol.*, **112**,199-221.

McNaughton, K.G., 2006. On the kinetic energy budget of the unstable atmospheric surface layer. *Bound.-Layer Meteorol.*, **118**, 83-107.

McNaughton, K.G. and Y. Brunet, 2002: Townsend's hypothesis, coherent structures and Monin-Obukhov similarity. *Bound.-Layer Meteorol.*, **102**, 161-175.

McNaughton, K.G. and J. Laubach, 2000: Power spectra and cospectra for wind and scalars in a disturbed surface layer at the base of an advective inversion. *Bound.-Layer Meteorol.*, **96**, 143-185.

Mehta, R.D. and P. Bradshaw, 1988: Longitudinal vortices embedded in turbulent boundary layers Part 2. Vortex pair with ‘common flow’ upwards. *J. Fluid Mech*., **188**, 529-546.

Obukhov, A.M., 1946: ‘Turbulence in an atmosphere with a non-uniform temperature.’ *Tr. Akad. Nauk. SSSR Inst. Teoret. Geofiz.*, No 1. (English translation in *Bound.-Layer Meteorol.* **2**, 2-29, 1971).

Priestley, C.H.B., 1954: Convection from a large horizontal surface. *Aust. J. Physics*, **7**,176-201.

Priestley, C.H.B., 1955: Free and forced convection in the atmosphere near the ground. *Quart. J. Roy. Meteorol. Soc.*, **81**, 139-143.

Puthenveettil, B.A. and J.H. Arakeri, 2005: Plume structure in high-Rayleigh number convection. *J. Fluid Mech.* **542**, 217-249.

Sreenivasan, K.R., 1995: On the universality of the Kolmogorov constant. *Physics of Fluids*, **11**, 2778-2784.

Wyngaard, J.C., O.M. Coté and Y. Izumi, 1971: Local free convection, similarity, and the budgets of shear stress and heat flux. *J. Atmos. Sci.*, **28**, 1171-1182.

Zhuang, Y., 1995: Dynamics and energetics of convective plumes in the atmospheric surface layer. *J. Atmos. Sci.*, **52**, 1712-1722.